Detailed scaling analysis of low-force polyelectrolyte elasticity

D. B. McIntosh,[1] N. Ribeck,[1] and O. A. Saleh[2,*]
[1]*Physics Department, University of California, Santa Barbara, California 93106, USA*
[2]*Materials Department and BMSE Program, University of California, Santa Barbara, California 93106, USA*
(Received 29 May 2009; published 7 October 2009)

Single-molecule force-extension data are typically compared to ideal models of polymer behavior that ignore the effects of self-avoidance. Here, we demonstrate a link between single-molecule data and the scaling pictures of a real polymer. We measure a low-force elasticity regime where the extension L of chemically denatured single-stranded DNA grows as a power law with force f: $L \sim f^{\gamma}$, with $\gamma \approx 0.60-0.69$. This compares favorably with the "tensile-blob" model of a self-avoiding polymer, which predicts $\gamma = 2/3$. We show that the transition out of the low-force regime is highly salt dependent, and use the tensile-blob model to relate this effect to the salt dependence of the polymer's Kuhn length and excluded-volume parameter. We find that, contrary to the well-known Odijk-Skolnick-Fixman theory, the Kuhn length of single-stranded DNA is linearly proportional to the Debye length of the solution. Finally, we show that the low-force elasticity becomes linear ($\gamma = 1$) at ≈ 3 M salt, and interpret this as a Θ point of the polymer. At this point, the force-extension data is best described by the wormlike chain model, from which we estimate the bare (nonelectrostatic) persistence length of the polymer to be ≈ 0.6 nm.

DOI: 10.1103/PhysRevE.80.041803 PACS number(s): 82.35.Rs, 82.37.Rs, 87.15.La

I. INTRODUCTION

Single-molecule manipulation experiments, in which a single polymer is stretched with a known force while its extension is measured, are direct probes of polymer elasticity. The elasticity of a polymer depends sensitively on the configurations it is allowed by the interactions between its monomers; these interactions are indicative of the physical and structural properties of the monomers. Thus, through proper modeling, single-molecule force-extension data can be related to the microscopic physical properties of the studied polymer. The success of this strategy is highly dependent on the choice of model linking elasticity to microscopic behavior. In the majority of work to date, the models chosen only describe ideal polymer behavior—that is, the models account for the short-range monomer interactions that give the polymer a local stiffness, but ignore interactions between monomers well-separated on the chain. Typical ideal models are the freely jointed chain (FJC), where the polymer consists of M rigid Kuhn segments of length l connected by flexible joints [1], and the wormlike chain (WLC), where the polymer is modeled as a continuous elastic rod with persistence length l_p [2]. Ideal models have been used to describe the elasticity of a variety of synthetic and biological polymers, including the notable success of the WLC model in describing the force-extension data of double-stranded DNA (dsDNA) over a wide range of solution conditions [2–4].

From a polymer physics viewpoint, the widespread success of ideal models in describing force-extension data is somewhat unexpected since long-range interactions can typically only be ignored under very specific (Θ) solvent conditions [1]. However, their use is justified by the role of the applied force in screening long-range interactions: the force f creates a "tensile screening length" $\xi \sim T/f$, where T is the thermal energy. Loops of length greater than ξ will be suppressed by the applied force; thus, long-range interactions will be disallowed on those length scales. If $\xi < l$, long-range interactions will be removed for all length scales, and ideal behavior should result. Indeed, almost all single-molecule pulling experiments have been performed in the $\xi < l$ regime, either because the apparatus is limited to applying high ($f > 10$ pN) forces, or because the polymer is very stiff (as is the case for dsDNA, with $l \approx 100$ nm). Notably, several experiments on highly flexible single-stranded nucleic acids (ssNAs) [5–7] have seen clear deviations from simple ideal force-extension behavior, a signature of the $\xi > l$ regime. However, no quantitative connection was made between this data and theories of real (non-ideal) polymers.

Here, we show an explicit link between single-molecule force-extension data and scaling pictures of real polymers. In Sec. II we review the scaling predictions for the elasticity of real polymers. In Sec. III we present force-extension data on chemically denatured single-stranded DNA (d-ssDNA), showing in Sec. III B how different elastic regimes in the data are linked to the scaling predictions. Section III C investigates the measured variation of the elastic behavior with the concentration of monovalent salt; some salt dependence is expected due to ssDNA's high charge. We relate the data to theories of the salt-dependent persistence length of a charged polymer. Finally, in Sec. III D we show that d-ssDNA reverts to ideal behavior at high salt; we interpret this as a Θ point, and use it to determine the bare (nonelectrostatic) persistence length of the polymer. Beyond this salt concentration, we show that d-ssDNA aggregates as predicted for a polymer in a poor solvent. Much of the data presented here was first announced in Ref. [8]; in comparison, this article contains more detailed methods, and more complete discussions of both the scaling picture and of relevant prior results.

II. SCALING THEORY

We consider an isolated polymer in a good solvent, initially in the absence of applied force. The polymer is mod-

*Email address: saleh@engineering.ucsb.edu

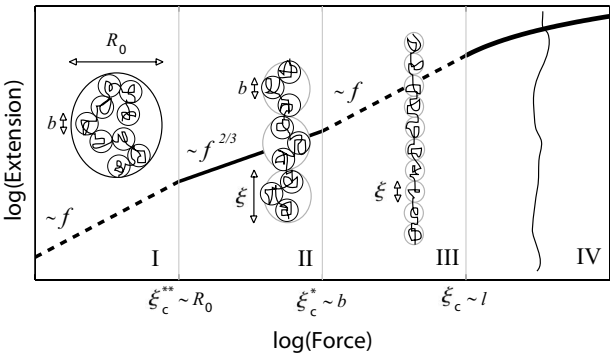

FIG. 1. Scaling predictions for the force-extension curve of a real semiflexible polymer in a good solvent. Regimes I and III are demarcated with dotted lines as these regimes are not seen in the data. The force-extension predictions in regimes I-III are simple power laws. In regime IV, the WLC model works for dsDNA [3], but our data on d-ssDNA show a logarithmic behavior that is not well understood. See text for details.

eled as a chain of M statistical monomers each having a Kuhn length l, where the contour length $L_0 \equiv Ml$. Following Flory, the rms size of the chain, R_0, is obtained by balancing the chain's entropy with the repulsive two-body monomer interactions parameterized by the excluded volume v [9],

$$R_0 \sim L_0^{3/5}\left(\frac{v}{l}\right)^{1/5}. \tag{1}$$

A simple scaling argument gives the dependence of the end-to-end extension L upon an applied tensile force f [10]: since R_0 is the characteristic length of the polymer, L should scale with R_0 and a function of the dimensionless ratio R_0/ξ. In particular, we take $L \sim R_0 \Psi(R_0/\xi)$, where the scaling function $\Psi(x)$ has different forms for different regimes of ξ. Following Netz [11], we anticipate up to four possible regimes of behavior (Fig. 1).

The lowest force regime (regime I) is defined by $\xi > R_0$. Here, the random-walk polymer is only slightly perturbed by the applied force, and linear response, $L \sim f$, should hold. This occurs if $\Psi(x) \sim x$, giving $L \sim R_0^2 f/T$. In regime I, the extension L grows as $L_0^{6/5}$ (i.e., faster than linear), indicating the importance of swelling [10].

As the force is increased, the contribution of swelling decreases until, at a crossover point $\xi_c^{**} \sim R_0$ or $f_c^{**} \sim T/R_0$, the polymer becomes strongly stretched ($L \sim L_0$). To satisfy the constraint of strong stretching, and given Eq. (1), requires $\Psi(x) \sim x^{2/3}$; thus the regime II force-extension behavior is

$$L \sim L_0\left(\frac{v}{l}\right)^{1/3}\left(\frac{f}{T}\right)^{2/3}. \tag{2}$$

Equation (2) depends on the Flory relation [Eq. (1)], thus it holds only when significant monomer interactions are present. In regime II, these interactions occur within subsections of the polymer ("tensile blobs") that adopt a self-avoiding random-walk structure on length scales less than ξ.

Further increase of the force decreases ξ until the tensile blobs contain too few monomers to be appreciably swollen, and Eq. (2) will no longer apply. A transition will occur when the excluded-volume contribution to the free energy per blob decreases to T, i.e., at a crossover point $\xi_c^* \sim b$, where b is the "thermal blob" size. For a semiflexible polymer with cylindrical monomers of length l and diameter $d < l$ (and, thus, $v < l^3$), $b \sim l^4/v$ [1]. Thus, the transition from regime II to III will occur at

$$f_c^* \sim Tv/l^4. \tag{3}$$

Within regime III, excluded-volume interactions are negligible, so the blobs behave as ideal coils of size ξ, and a linear force-extension relation is expected.

A final crossover should occur when $\xi_c \sim l$, or

$$f_c \sim T/l. \tag{4}$$

Above f_c (in regime IV), the polymer is highly aligned: the large tension does not permit the polymer to form loops. This can be contrasted with regime III, where some loops can form, but the resulting long-range interactions are too few to affect the polymer configuration. The lack of long-loop interactions in regime IV leads to the simple expectation that the force-extension behavior might display ideal elasticity; however, as described below, the measured behavior does not conform to the FJC or WLC predictions.

All told, scaling theory predicts up to four regimes in a force-extension curve (see Fig. 1): I. a single slightly stretched self-avoiding blob ($L \sim f$) for $f < T/R_0$; II. a chain of self-avoiding tensile blobs ($L \sim f^{2/3}$) for $T/R_0 < f < T/b$; III. a chain of ideal thermal blobs ($L \sim f$) for $T/b < f < T/l$; and IV. a chain of nearly aligned monomers for $T/l < f$ [11].

As described below, regime III does not appear in the data. We conclude that this is because l does not differ significantly from d in our conditions, and thus that this regime is vanishingly small ($T/b \approx T/l$). Instead, we observe regime II transitioning directly into regime IV. That transition takes place at a crossover force given by Eq. (4); thus, according to Eq. (2), the crossover length, L_c, between these two regimes will be

$$L_c/L_0 \sim (v/l^3)^{1/3}. \tag{5}$$

Since we independently measure f_c and L_c/L_0, we can use Eq. (4) and (5) to estimate v and l from our data without assuming a relation between v and l.

III. FORCE-EXTENSION MEASUREMENTS

A. Methods

In order to access force regimes $\xi \gtrsim l$, we need an apparatus capable of stretching polymers with low forces and a polymer with short Kuhn length l and a statistically significant number of monomers M. The former criteria is met by using magnetic tweezers while the latter is met by using long strands of denatured single-stranded DNA (d-ssDNA). Magnetic tweezers are unique single-molecule stretching apparatuses in that they intrinsically apply constant force (i.e., they are force-clamps, not position-clamps). In short, magnetic tweezers protocol consists of tethering a single polymer molecule between a glass surface and a small paramagnetic bead

and using the position of external, macroscopic magnets to control the force applied to this bead [12]. As such, we can exert arbitrarily small forces on the tethered polymer by simply moving the magnets far from the sample, limited only by difficulties encountered when the bead interacts frequently with the glass surface.

Single-stranded nucleic acids (ssNAs) are polymers with Kuhn lengths of order a few nanometers [5–7], and long ssNAs (with $M \gtrsim 10^4$) are easily generated by enzymatic methods and/or denaturation of dsDNA. Labeled ssDNAs are primarily generated by PCR amplification of a 10.5 kbp segment of the Lambda phage genome using 5′ biotin labeled primers and 3′ digoxigenin labeling using terminal transferase. Additional control experiments are performed using the entire 48.5 kbp Lambda phage genome. This longer substrate is prepared by ligating biotin and digoxigenin labeled oligos to the *cos* sequences of the Lambda template. The use of ssNAs is complicated by the possible formation of secondary structure by intrastrand base pairing. Here, base pairing is avoided by permanent chemical denaturation: dsDNA is first thermally denatured at 95 °C to form ssDNA, then base pairing is inhibited by reaction with 1 M glyoxal for 1 h at 50 °C [13].

Single-molecule tethers are formed by first mixing labeled d-ssDNA with an excess of antidigoxigenin, then flowing ~10 pM of antibody/d-ssDNA complexes into a glass flow cell. The complexes attach to the glass through nonspecific adsorption of the antibody. The glass is then passivated with a solution containing 0.1% Tween 20 and 0.1% F-127 Pluronics, after which Streptavidin-coated magnetic beads are bound to the biotin labels. Some d-ssDNA tethers prepared in this fashion are shorter than expected. While we originally attributed this to intrastrand glyoxal cross linking [8], we have since determined it is due to nonspecific binding of the d-ssDNA to the glass (this difference does not affect any of our prior conclusions). Thus, we developed an alternative passivation method: incubate the surface with 20 μg/mL antidigoxigenin, passivate with 0.1 mg/mL glyoxal-treated, sonicated herring sperm DNA and 1 mg/mL Bovine Serum Albumin, add ≈100 pM d-ssDNA tethers, then bind magnetic beads. We find this method appreciably reduces the fraction of short tethers. All data presented here for the longer DNA substrate were taken using this latter protocol.

Force-extension data are acquired using standard magnetic-tweezer protocols: We use an external magnetic field to apply a force to the tethered magnetic beads, stretching the ssDNA. Optical bead tracking is used to measure extension and force, as described in Ref. [12]. Experiments were performed in a sodium phosphate buffer, pH ≈ 6.5; NaCl was added to the buffer to obtain the desired monovalent salt concentration c.

B. Two force regimes

All force-extension curves in solutions of moderate salt concentration, 20 mM ≤ c ≤ 2 M, exhibit two regimes demarcated by a crossover force, f_c (Fig. 2). For forces $f < f_c$, the extension L increases as a power law, while for forces $f > f_c$, L increases logarithmically (sub-power law) with f. At higher salt concentrations, we find that the low-force regime persists to larger forces resulting in a larger f_c. Salt concentrations $c < 20$ mM resulted in logarithmic force-extension curves over the entire accessible force range. Presumably, the power-law regime exists at these low salt concentrations, but ends at forces too small to measure; that is, $f_c < 0.1$ pN in low salt conditions. For $c < 2$ M, we do not observe extension to depend linearly on force for any value of f. We conclude that both regime I (linear response) and regime III (thermal blobs) are inaccessible in this experiment. Regime I presumably occurs at forces too low to access in our setup. As argued above, and in Ref. [11], the absence of regime III indicates that the statistical monomers are more spherelike ($l \approx d$) than rodlike ($l \gg d$).

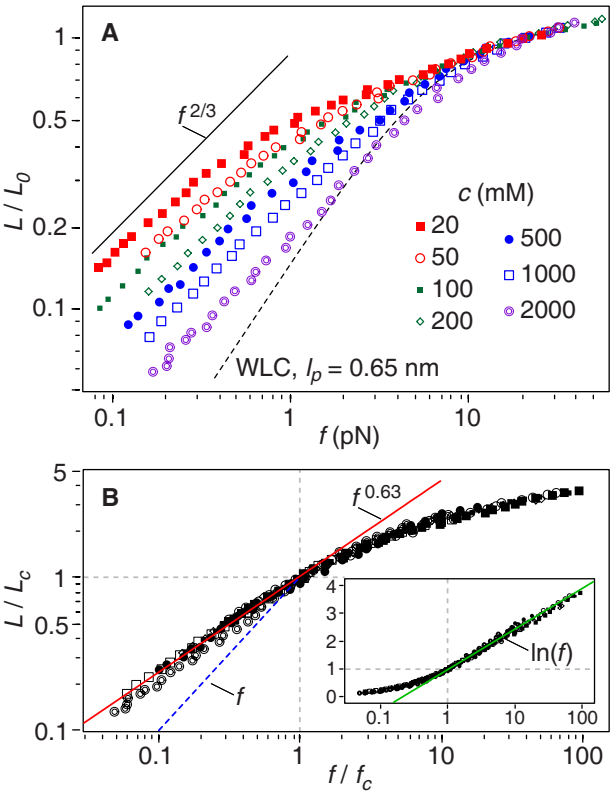

FIG. 2. (Color online) Figure reproduced from Ref. [8]. (A) Representative data of relative length (scaled by $L_0 \approx L(f=20$ pN); see text) vs. force for d-ssDNA at various salt concentrations. The solid line indicates the slope of the predicted power law, Eq. (2), and the dashed line is the WLC prediction with $l_p = 0.65$ nm. (B) Data from (A) between 20 mM and 2 M replotted with L and f scaled by the crossover values L_c and f_c. The solid line is the power-law $L \sim f^{0.63}$, while the dashed line is a linear curve. Inset: The same data, plotted on lin-log axes to emphasize the high-force logarithmic behavior; the line indicates $L \sim 0.63 \ln(f)$.

For each force-extension curve, we isolate the low-force regime, fit $L \sim f^{\gamma}$, and examine the dependence of γ on c (Fig. 3). For 20 mM ≤ c ≤ 2 M, γ is relatively constant, varying from ≈0.6 to ≈0.69. At these salt concentrations, the value of γ compares well with the scaling prediction from Eq. (2). Thus, we conclude that the low-force regime measured here corresponds to the self-avoiding tensile-blob regime discussed above (regime II).

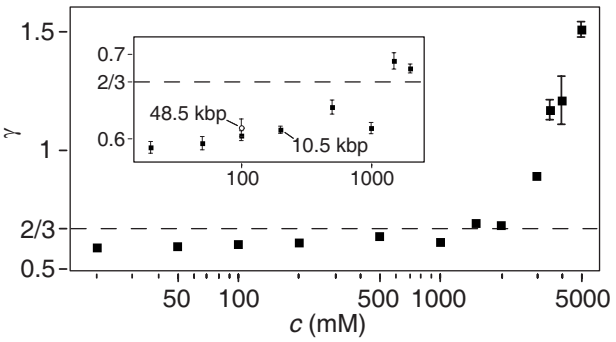

FIG. 3. Measured power-law exponent γ vs salt concentration c from 55 force-extension curves, with between two and ten curves averaged per point. Figure data on 10.5 kbp substrate reproduced from Ref. [8]. Inset: detail of the regime 20 mM$\leq c \leq$2 M, with labels indicating the substrate used.

For $c<1$ M, the measured value of γ is consistently lower than the prediction. In recent theoretical work, Morrison *et al.* [14] found a similar deviation, and attributed it to a slight stretching within the tensile blobs by the applied force. Their work predicts that the deviation should disappear for sufficiently long polymers [14]; thus, we investigated the contour-length dependence of the exponent. Five force-extension curves were taken on the 48.5 kbp substrate at $c=100$ mM. For the longer substrates, the fit value of γ is still below 2/3 (see Fig. 3). However, this does not rule out the existence of a finite-length effect: Morrison *et al.* found $\gamma \approx 2/3$ only for chains with $M \gtrsim 10^5$ [14]. In our experiments with the longer substrate ($L_o \approx 25$ μm) and assuming a Kuhn length $l \approx 1$ nm (likely a slight underestimate; see below), the polymer has $M \approx 10^4$. We conclude that observing the precise exponent $\gamma=2/3$ requires ssDNA molecules roughly tenfold longer than those used here (i.e., several hundred kbp, corresponding to contour lengths of a few hundred microns); our current experimental methods do not permit the manipulation of such huge substrates.

A logarithmic regime has been observed in previous force-extension data on ssNAs [6,7,15] and in one study on spider-silk protein [16]. The logarithmic regime is permitted by scaling theory [8], but determining the microscopic mechanism that gives rise to the logarithm is difficult. The lack of excluded-volume interactions for $f>f_c$ implies that the elasticity depends only on local stiffness, and thus that ideal force-extension predictions should describe the data. However, the data from both our work and prior studies [6,7] coincide with simple FJC and WLC predictions only for a limited range of moderately high forces. It is likely that one or more other mechanisms are needed to explain the data. Several possibilities exist in the literature, including polymer extensibility (stretch elasticity) [5,6,17], and the interplay between the tension derived from applied force and that derived from electrostatic repulsion between monomers [11]. One mechanism shown to play a role is the so-called scale dependence of the persistence length: Barrat and Joanny [18] calculated that the contribution of the electrostatic repulsion to the polymer's persistence length is dependent on the wavelength of the bending fluctuations. Building on this work, Marko and Siggia [2] pointed out that, under applied tension, there is a force-dependent cutoff of long-wavelength fluctuations, and thus a force dependence to the persistence length. They proposed a calculation strategy to incorporate scale dependence into a WLC-based force-extension prediction valid in the highly stretched ($L/L_0>0.5$) regime [2]. Using this strategy we find agreement over a larger range of forces than the simple WLC prediction (data not shown); a similar conclusion was found previously for ssRNA [7]. However, the agreement is still incomplete. This is expected, as the logarithmic behavior persists to lower extensions ($L/L_0<0.5$) than described by the theory.

C. Effect of salt

Over two decades in monovalent salt concentration, 20 mM$\leq c \leq$2 M, all force-extension curves display a low-force power law (with exponent $\gamma \approx 2/3$) and a high-force logarithm. The principal effect of changing c is to change the crossover point between the two regimes. To quantify this dependence, we extract the crossover point (f_c, L_c) from each curve by fitting to a single relation that is both continuous and smooth at the crossover point,

$$L = L_c(f/f_c)^{\gamma} H(f_c - f) + L_c[\gamma \ln(f/f_c) + 1] H(f - f_c), \quad (6)$$

where the step function $H(x)=0(1)$ for $x<0(\geq 0)$. We fixed γ to the value found from power-law fits at each c, and fit Eq. (6) to each curve using only two free parameters, f_c and L_c. Universal behavior for this range of salt concentrations is demonstrated by the collapse of all force-extension data when scaled by the fit values of f_c and L_c [Fig. 2(B)].

The results of Sec. II indicate that we can use the fit values of f_c and L_c to estimate the dependence of l and υ on c by applying Eqs. (4) and (5). To do so requires an estimate of L_0. In typical force-extension data, L_0 is extracted from fits to a WLC or FJC model. Since these models are inconsistent with the observed high-force logarithmic behavior, and since we lack an alternate model for that behavior, we extract a model-independent estimate for L_0 from each force-extension curve by interpolating the extension at 20 pN, and setting $L_0=L(f=20$ pN). Above 20 pN, the salt-dependent effects of the force-extension data disappear [Fig. 2(A)]. Alternative estimates of L_0 based on fitting high-force data ($f>10$, 20 or 30 pN) to either extensible-FJC or WLC modes resulted in contour lengths that differ from our estimate by a multiplicative factor constant for all c. Since our analysis ignores prefactors, this absolute variation is unimportant, and we use $L_0=L(20$ pN) throughout.

In the range 20 mM$\leq c \leq$2 M, we find both f_c and the ratio L_c/L_0 increase monotonically with c (Fig. 4); power-law fits give $f_c \sim c^{0.54\pm0.03}$ and $L_c/L_0 \sim c^{0.11\pm0.01}$. From the f_c and L_c/L_0 power laws, we estimate the salt concentration dependence of l and υ using Eqs. (4) and (5) (Fig. 4). The best-fit power-law dependence of the Kuhn length and excluded-volume parameters are $l \sim c^{-0.51\pm0.04}$ and $\upsilon \sim c^{-1.09\pm0.17}$ [35], respectively.

Electrostatic repulsion between charged monomers tends to increase the local stiffness of a charged polymer. In salty solution, the electrostatic potential is exponentially screened over the Debye length, $\lambda_D \sim c^{-0.5}$; thus, a relationship be-

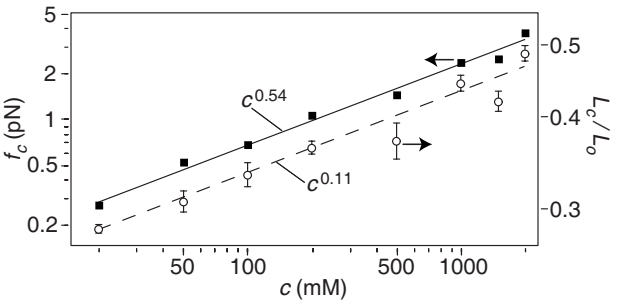

FIG. 4. Figure reproduced from Ref. [8]. The crossover force, f_c (filled squares), and the relative crossover length, L_c/L_0 (open circles), vs salt concentration c. The data are from 54 force-extension curves, with between two and ten curves averaged per point. The continuous (dashed) line is the best-fit power law to the f_c (L_c/L_0) data, with exponent as shown.

tween l and λ_D is expected. Indeed, such a relationship was found in the Odijk-Skolnick-Fixman (OSF) calculation, in which the enthalpy of a charged rod is calculated as a function of its curvature [19,20]. In this formulation, the resulting Kuhn length is written as the sum of a bare or structural component (l_0) and an electrostatic component (l_e): $l=l_0+l_e$. OSF theory predicts that $l_e \sim \lambda_D^2$, conflicting with our result of $l_e \sim \lambda_D$. Similar experiments on dsDNA, however, agree with the OSF prediction [4]. These different results are likely due to the differences between the two polymers: dsDNA is both torsionally constrained and highly stiff, forcing measurements to be in the regime where $\lambda_D \ll l_0$ and $\xi < l$. In contrast, our work with d-ssDNA (a torsionally free, flexible polymer) is in the regimes $\lambda_D \gtrsim l_0$ and $\lambda_D \lesssim l_0$. Further, we access forces for which $\xi \gtrsim l$. Certain theoretical results are able to reconcile the experiments: OSF theory was modified to introduce configurational fluctuations by Barrat and Joanny, who predict $l_e \sim \lambda_D^2$ for stiff polymers and $l_e \sim \lambda_D$ for flexible polymers, consistent with both experiments [18]. More recently, Dobrynin noted that OSF theory, by considering polymer conformations restricted to a single plane, ignored torsional fluctuations, and thus might only apply to torsionally constrained polymers such as dsDNA. Including torsional freedom in the OSF calculation gives $l_e \sim \lambda_D$, also consistent with our result [21].

Several other experiments on flexible polyelectrolytes have estimated the dependence of l_e on c [22–25]. Tinland *et al.* analyzed measurements of the diffusion coefficients of ssDNA in high concentrations of the denaturant urea to find $l_e \sim \lambda_D$ [22]. Viscometry and static light-scattering experiments on other flexible polyelectrolytes have resulted in similar contradictions to the OSF theory [23,24]. Conversely, small-angle x-ray studies of unfolded ssRNA found $l_e \sim \lambda_D^2$, in agreement with the OSF result [25]. In bulk measurements, excluded-volume effects are either neglected (see [22,23,25]) or significantly complicate the analysis (as in [24]). Our method directly accounts for excluded-volume effects, resulting in an estimate for the scaling of v with c. Furthermore, compared to these bulk studies, our work has the advantage of relying on a relatively simple, robust scaling argument [particularly Eq. (4)] rather than the more model-dependent assumptions used to extract l from the data in Refs. [22–25].

Both l and v are estimates of the effective size (including electrostatic effects) of the statistical monomers, thus a relation between them is expected. The estimated salt dependences, $l \sim c^{-0.51 \pm 0.04}$ and $v \sim c^{-1.09 \pm 0.17}$, are consistent with $v \sim l^2 d$, as predicted for cylindrical monomers of length l and diameter d [26], if we assume d is independent of salt concentration. This is likely a good assumption: we expect d to depend on λ_D and the steric diameter (≈ 1 nm) of the polymer. In the range of salt we utilize ($c \geq 20$ mM), $\lambda_D \leq 2.2$ nm, thus the electrostatic contribution is at best comparable (and, for most of the range, less than) the steric size. However, the relation $v \sim l^2 d$ is only expected in the limit $d \ll l$ [26]. Our result $l \sim \lambda_D$, with $\lambda_D \leq 2.2$ nm, indicates instead that d and l are comparable in this study. The general dependence of v on l is not a simple power law: $v \sim l^\alpha d^{3-\alpha}$ where the exponent α is itself a function of the ratio d/l [26]. Thus, quantitatively relating v to l requires precise knowledge of the relation of d to l; since our analysis permits neither an estimate of d, nor a numerically precise estimate of l, we are unable to draw a clear conclusion.

D. Theta point

While relatively stable for $c < 2$ M, the low-force power-law exponent γ increases for $c > 2$ M, reaching $\gamma \approx 1$ at $c \approx 3$ M (Fig. 3). A broad linear regime is expected for an ideal polymer: repeating the scaling argument of Sec. II that led to the $L \sim f^{2/3}$ prediction [Eq. (2)], but starting instead with the nonswollen random-walk relation $R_0 \sim M^{1/2}$, results in a linear force-extension relation. Thus, we interpret $c \approx 3$ M as a Θ point of d-ssDNA: At this high salt concentration, electrostatic repulsion is screened to the extent that it is statistically compensated for by weak attractive forces (e.g., van der Waals or hydrophobic interactions), causing the excluded-volume parameter to vanish ($v=0$). This interpretation is consistent with prior sedimentation and light-scattering studies that found Θ points for ssNAs at $c \approx 1-2$ M [27–29].

If $c \approx 3$ M is a Θ point, then the increased screening at $c > 3$ M should lead to monomer aggregation. Indeed, we observe evidence of this: the extension changes rapidly at low forces for these salt concentrations (Fig. 5) resulting in $\gamma > 1$ for $c > 3$ M (Fig. 3), indicating the presence of aggregates that break apart under applied force. The measured values reach $\gamma \approx 1.5$ at the limit set by the solubility of the salt, and are still increasing at that point.

The Θ condition at $c=3$ M allows us to evaluate the applicability of force-extension predictions of the ideal FJC [5] and WLC [2] models. For both models, the predictions fit two parameters including the contour length L_0 and the Kuhn length l (for the FJC) or persistence length $l_p = l/2$ (for the WLC). Either model can be modified to account for stretching of the phosphate backbone by adding a third parameter (the stretch modulus K). These models are referred to as the extensible-FJC (EFJC) or extensible-WLC (EWLC). We find that the FJC prediction does not adequately fit the data, while the EWLC fits do not significantly improve the WLC fits; thus, we do not consider them further. WLC fits produce χ^2 values $\approx 15\%$ better than the EFJC fits, despite having one

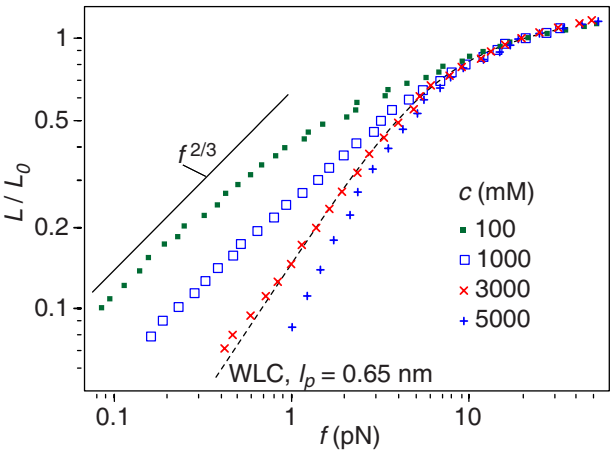

FIG. 5. (Color online) Representative force-extension curves in good ($c=100$ and 1000 mM), near-Θ (3000 mM), and poor (5000 mM) solvents. At the Θ point, the data are best fit by the WLC model; for the curve shown, the best-fit persistence length is 0.65 nm.

fewer parameter. Further, the EFJC fits produce values of $K \approx 200$ pN, anomalously low compared to the values found in higher-force experiments [5,15]. We conclude that the WLC model provides a better description of the elasticity of d-ssDNA at the Θ point.

The value of the persistence length, $l_{p,\Theta}$, that we extract from WLC fits at the Θ point is indicative of d-ssDNA's nonelectrostatic structural stiffness l_0. Averaged over three curves, we find $l_{p,\Theta}=0.62\pm0.01$ nm, and thus a bare Kuhn length $l_0=1.24\pm0.02$ nm. The fit value of $l_{p,\Theta}$ is similar to the spacing of ≈0.5–0.7 nm between ssNA bases [30]. Such a small persistence length calls into question the WLC's assumption of continuous elasticity. Applicability of the WLC to d-ssDNA elasticity might be explained by the complexity of the polymer backbone: each base is separated by multiple bonds whose combined configurational freedom might approximate continuous elasticity. This explanation is supported by Livadaru *et al.*, who predict that a polymer with discrete bonds of length a will display WLC-like continuous elastic behavior for $f<Tl_p/a^2$ [31]. Here, using $a\approx0.1$ nm, this corresponds to forces below ≈250 pN; since the maximum force in our data is ≈50 pN, our results agree with that prediction. Generally, it is likely that both the FJC and WLC models are best viewed as limiting cases of, respectively, discrete and continuous elasticity, and that a full description of polymer elasticity requires a mixture of both, as attempted in recent theories [17,31].

Similar persistence lengths have been measured in other pulling experiments on ssNAs. Smith *et al.* used high-force data on nondenatured ssDNA to estimate the persistence length by fitting to an EFJC model and obtained $l_p=0.75$ nm [5], in relatively good agreement with our results. Recent experiments on homopolymeric single-stranded RNA estimate that $l_{p,\Theta}=1.03\pm0.02$ nm [7], although the Θ condition was not definitively established in that work. The higher value for ssRNA vs. ssDNA is consistent with ssRNA's reduced configurational freedom due to the steric hindrance of the additional oxygen on RNA's backbone [7].

While our result for $l_{p,\Theta}$ is similar to other single-molecule pulling experiments, it is smaller than that found in most bulk measurements. In a series of papers, Felsenfeld and collaborators investigated the Flory characteristic ratio of ssNAs in Θ solvents by sedimentation and light-scattering experiments [27–29]. That data was interpreted by Mills *et al.* to correspond to $l_{p,\Theta}\approx1.0-1.5$ nm [30]. Mills *et al.* also provide independent estimates of l_p of ssDNA based on measurements of rotational diffusion times of gapped duplex DNA (two dsDNAs connected by a 12 or 24 base ssDNA). Their data show a regime with no salt dependence; while not strictly a Θ point, they argue that the behavior of the complex in this regime corresponds to the intrinsic rigidity of the ssDNA, and report $l_p\approx2-3$ nm [30]. Rivetti *et al.* [32] used AFM imaging to estimate the persistence length of ssDNA oligos from similar gapped dsDNA duplexes and found $l_p\approx1.3$ nm, also larger than our result. The discrepancy between our results and those on gapped duplexes can likely be attributed to differences in the electrostatic environment of the measured ssDNAs, particularly due to the interaction between the relatively short ssDNA and the dsDNA attached on each side. Supporting this, Jose *et al.* recently observed that the structural properties of bases neighboring ds/ssDNA junctions deviate from bases in the middle of an ssDNA strand [33]. Such anomalies perhaps explain why Mills *et al.* observe a saturation of salt-dependent effects above 60 mM NaCl [30] while we find that l is modulated by salt throughout the entire range 20 mM$\leq c\leq$5 M. More generally, our approach is relatively simple in comparison with most bulk studies; thus our estimate of $l_{p,\Theta}$ is likely the most direct to date.

IV. CONCLUSION

We provide an in-depth examination of the elasticity of a polymer in a good solvent as predicted by scaling theory, and reconcile these predictions with single-molecule force-extension data. By examining the low-force behavior of chemically denatured ssDNA, our work reveals a nonlinear power-law regime (regime II) previously predicted, but not observed. By analyzing the salt dependence of the crossover from this power-law regime to a fully stretched logarithmic regime, we find that the Kuhn length of d-ssDNA is proportional to the solution's Debye length. Finally, upon increasing the NaCl concentration to ≈3 M, we find that the net monomer repulsion is screened away and the polymer behaves ideally. We identify this as a Θ condition for d-ssDNA and find that the data are best fit by the predictions of the ideal WLC model with persistence length $l_{p,\Theta}=0.62\pm0.01$ nm.

While we have shown evidence that our experiment accesses the tensile-blob regime (regime II) of the scaling picture presented in Sec. II and Ref. [11], we are not able to access regimes I or III. For what range of parameters might these regimes be observed? Regime I corresponds to linear response, and occurs only for $f<f_c^{**}\sim T/R_0$. The extension at crossover into regime I is $L_c^{**}\sim R_0$. In our experimental apparatus, where the polymer is tethered between a relatively large bead and a planar glass surface, such small extensions

would force the polymer to have significant excluded-volume interactions with the bead and surface, severely altering its configurational freedom and complicating the analysis. Thus, observing regime I is unlikely in standard single-molecule manipulation setups. Regime III occurs for forces $T/b<f<T/l$, thus observation of regime III alone requires that the polymer have significant separation between its Kuhn length and thermal blob size: $l \ll b$. Since $b \sim l$ for spherical monomers, this conditions requires cylindrical monomers with $d \ll l$. dsDNA (with $l \approx 100$ nm and $d \approx 2$ nm) meets this condition, but the large value of l means that regime III occurs only for $f<0.04$ pN, at the edge of the accessible regime in single-molecule manipulation techniques. Instead, a polymer with cylindrical monomers of $l \approx 10$ nm (given $d \approx 1$ nm) would give a crossover from III to IV at an achievable $f_c \approx 0.4$ pN; certain ssNA homopolymers, where base-stacking interactions increase l over the value measured here [30,34], could fit this condition. Ideally, the crossover at f_c^* from regime II to III would also be observable in the same experiment; however, given $l \approx 10$ nm and $d \approx 1$ nm, we have $f_c^* \approx 0.04$ pN, again at the limit of the technique.

Our results suggest two future directions of research. First, the logarithmic force-extension regime observed here (and previously in Refs. [6,16]) is not well understood; theoretical work is needed to determine the microscopic mechanism that accounts for this regime. Second, we focus here on monovalent salt solutions, and compare our results to the various theories relating the electrostatic persistence length to c. This is consistent, as those theories rely on the Debye-Huckel approximation that is only quantitatively accurate for monovalent salt. It is clearly of interest, and experimentally feasible, to test solutions of multivalent salts for which the theoretical assumptions break down.

ACKNOWLEDGMENTS

We thank P. Pincus and D. Thirumalai for helpful conversations. This work was supported by the National Science Foundation under Grant No. PHY-0748564 and by the MRSEC Program under Award No. DMR05-20415.

[1] M. Rubinstein and R. H. Colby, *Polymer Physics* (Oxford University Press, USA, 2003).
[2] J. F. Marko and E. D. Siggia, Macromolecules **28**, 8759 (1995).
[3] C. Bustamante, J. F. Marko, E. D. Siggia, and S. Smith, Science **265**, 1599 (1994).
[4] C. G. Baumann, S. B. Smith, V. A. Bloomfield, and C. Bustamante, Proc. Natl. Acad. Sci. U.S.A. **94**, 6185 (1997).
[5] S. B. Smith, Y. J. Cui, and C. Bustamante, Science **271**, 795 (1996).
[6] M. N. Dessinges, B. Maier, Y. Zhang, M. Peliti, D. Bensimon, and V. Croquette, Phys. Rev. Lett. **89**, 248102 (2002).
[7] Y. Seol, G. M. Skinner, and K. Visscher, Phys. Rev. Lett. **93**, 118102 (2004).
[8] O. A. Saleh, D. B. McIntosh, P. Pincus, and N. Ribeck, Phys. Rev. Lett. **102**, 068301 (2009).
[9] P. G. de Gennes, *Scaling Concepts in Polymer Physics* (Cornell University Press, Ithaca, NY, 1979).
[10] P. Pincus, Macromolecules **9**, 386 (1976).
[11] R. R. Netz, Macromolecules **34**, 7522 (2001).
[12] N. Ribeck and O. A. Saleh, Rev. Sci. Instrum. **79**, 094301 (2008), and references therein.
[13] G. K. McMaster and G. G. Carmichael, Proc. Natl. Acad. Sci. U.S.A. **74**, 4835 (1977).
[14] G. Morrison, C. Hyeon, N. M. Toan, B. Y. Ha, and D. Thirumalai, Macromolecules **40**, 7343 (2007).
[15] M. Rief, H. Clausen-Schaumann, and H. E. Gaub, Nat. Struct. Biol. **6**, 346 (1999).
[16] N. Becker, E. Oroudjev, S. Mutz, J. P. Cleveland, P. K. Hansma, C. Y. Hayashi, D. E. Makarov, and H. G. Hansma, Nature Mater. **2**, 278 (2003).
[17] C. Storm and P. C. Nelson, Phys. Rev. E **67**, 051906 (2003).
[18] J. L. Barrat and J. F. Joanny, Europhys. Lett. **24**, 333 (1993).
[19] T. Odijk J. Polym. Sci., Part B: Polym. Phys. **15**, 477 (1977).
[20] J. Skolnick and M. Fixman, Macromolecules **10**, 944 (1977).
[21] A. V. Dobrynin, Macromolecules **38**, 9304 (2005).
[22] B. Tinland, A. Pluen, J. Sturm, and G. Weill, Macromolecules **30**, 5763 (1997).
[23] M. Tricot, Macromolecules **17**, 1698 (1984).
[24] W. F. Reed, S. Ghosh, G. Medjahdi, and J. Francois, Macromolecules **24**, 6189 (1991).
[25] G. Caliskan, C. Hyeon, U. Perez-Salas, R. M. Briber, S. A. Woodson, and D. Thirumalai, Phys. Rev. Lett. **95**, 268303 (2005).
[26] L. Onsager, Ann. N. Y. Acad. Sci. **51**, 627 (1949).
[27] H. Eisenberg and G. Felsenfeld, J. Mol. Biol. **30**, 17 (1967).
[28] L. D. Inners and G. Felsenfeld, J. Mol. Biol. **50**, 373 (1970).
[29] E. K. Achter and G. Felsenfeld, Biopolymers **10**, 1625 (1971).
[30] J. B. Mills, E. Vacano, and P. J. Hagerman, J. Mol. Biol. **285**, 245 (1999).
[31] L. Livadaru, R. R. Netz, and H. J. Kreuzer, Macromolecules **36**, 3732 (2003).
[32] C. Rivetti, C. Walker, and C. Bustamante, J. Mol. Biol. **280**, 41 (1998).
[33] D. Jose, K. Datta, N. P. Johnson, and P. H. von Hippel, Proc. Natl. Acad. Sci. U.S.A. **106**, 4231 (2009).
[34] Y. Seol, G. M. Skinner, K. Visscher, A. Buhot, and A. Halperin, Phys. Rev. Lett. **98**, 158103 (2007).
[35] Equation (5) assumes $\gamma=2/3$, which differs slightly from the measured value (Fig. 3). However, we have found only a $\approx 10\%$ difference in the results depending on which exponent is used, thus we ignore the difference, and include the 10% in the estimated uncertainty.